In: Ordinary and Partial Differential Equations
Editor:
ISBN:

Chapter 1

SOLITARY WAVES IN THE NONLINEAR DIRAC EQUATION AT THE CONTINUUM LIMIT: STABILITY AND DYNAMICS

Jesús Cuevas–Maraver[1,2*]***, Panayotis G. Kevrekidis***[3,4]***, Avadh Saxena***[4]***,***
Fred Cooper[4,5] ***and Franz G. Mertens***[6]
[1]Grupo de Física No Lineal, Departamento de Física Aplicada I,
Universidad de Sevilla.
Escuela Politécnica Superior, C/ Virgen de África, 7, 41011-Sevilla, Spain
[2]Instituto de Matemáticas de la Universidad de Sevilla (IMUS).
Edificio Celestino Mutis. Avda. Reina Mercedes s/n, 41012-Sevilla, Spain
[3]Department of Mathematics and Statistics, University of Massachusetts,
Amherst, MA 01003-9305, USA
[4]Center for Nonlinear Studies and Theoretical Division,
Los Alamos National Laboratory, Los Alamos, New Mexico 87545, USA
[5]Santa Fe Institute, Santa Fe, NM 87501, USA
[6]Physikalisches Institut, Universität Bayreuth, D-95440 Bayreuth, Germany

Abstract

In the present work, we give a comparative summary of different recent contributions to the theme of the linear stability and nonlinear dynamics of solitary waves in the nonlinear Dirac equation in the form of the Gross-Neveu model. We indicate some of the key controversial statements in publications within the past few years and we attempt to address them to the best of our current understanding. The conclusion that we reach is that the solitary wave solution of the model is spectrally stable in the cubic nonlinearity case, however, it may become unstable through an instability amounting to the violation of the Vakhitov-Kolokolov criterion for higher exponents. We find that for the Dirac model, the interval of instability is narrower. A fundamental numerical finding of our work is that, contrary to what is the case in the nonlinear Schrödinger analogue of the model, the unstable dynamical evolution, does *not* lead to collapse (blowup) and hence it appears that the relativistic nature of the model mitigates the

*E-mail address: jcuevas@us.es

collapse instability. Various issues associated with different numerical schemes are highlighted and some possibilities for future alleviation of these is suggested.

PACS 05.45.Yv. **Keywords:** Solitons, nonlinear Dirac equation, stability, dynamics

1. Introduction

Variants of the nonlinear Dirac equation (NLDE) and special solitary wave solutions of this model have now been proposed for more than 50 years [1, 2]. In suitable non-relativistic limits [3], these models have also been connected to their far more widespread dispersive nonlinear wave analogue, namely the nonlinear Schrödinger equation (NLSE) [4, 5]. Nevertheless, it has turned out that the Dirac equation as a result of its matrix nature and the fact that it is only first order in spatial derivatives (as opposed to second order in the NLSE) has proven far more computationally (and theoretically) challenging, on a number of grounds, than its NLSE counterpart. For a summary of a number of the computational issues arising in this connection, the interested reader can refer to [6, 7, 8]. On the other hand, numerous mathematical works have attempted to address issues of orbital and asymptotic stability of solitary wave solutions in the model [9, 10, 11, 12], and different kinds of potential stability/instability criteria [13, 14].

Here, we will revisit this theme of stability and dynamics of the solutions of the NLDE, in the context of a concrete, well-established (especially in the context of high energy physics) model, namely the Gross-Neveu model [15]. This model has been generalized recently to arbitrary nonlinearity powers [8] (parametrized by an exponent k) and exact solitary wave solutions have been obtained. It is the linear (spectral) stability and nonlinear dynamics of such solutions that we will consider herein. We will discuss in the paper both the equation with cubic non-linearity ($k = 1$) as well as the case for arbitrary k.

It turns out that the question of stability and dynamics has been one which is highly controversial in recent years. Early work of Bogolubsky for the cubic nonlinearity case predicted that for frequencies below a critical one, instability should ensue [16]. On the contrary, the numerical (short time) simulations of Alvarez and Soler did not identify an instability and concluded stability for all frequencies Λ [17]. In [8], it was questioned whether the multi-hump solutions that arise for small values of Λ were associated with a stability change and, in fact, more recently in [18] and later in [7], it was argued based on Bogolubsky-type considerations and longer numerical simulations that an instability threshold does exist which was argued to be 0.6976 in [18] and 0.56 in [7]. These results, however, are in disagreement with the linear (spectral) stability calculations, of [19], based on the well established and highly accurate technique of the Evans function (identifying point spectrum eigenvalues and associated instabilities) [20]. They are also in disagreement with the conclusions of [21]. The latter explored the transverse instability of quasi-one-dimensional nonlinear waves in a 2d Dirac equation. In that setting, it was shown that for 1d perturbations (uniform in the transverse direction), the waves do not manifest a spectral instability in the Chebyshev collocation scheme utilized in that work. An instability of a centered-difference discretization scheme near the continuum limit was recently reported in [22], although the authors therein cautioned against the danger of extending these results (of the discrete context) all the way to the continuum limit.

Admittedly, the above conclusions may leave the reader rather in confusion, given the apparently contradictory nature of the obtained results. This, in turn, only attests to both the analytical (as no definitive analytical spectral result exists e.g. in the most highly discussed cubic, one-dimensional case) and numerical challenges raised by the present setting. Our aim in the present work is to shed some further light on this controversy, by testing and comparing different methods both for the stability properties of the continuum solutions and also for their nonlinear dynamics.

Our presentation will be structured as follows. In section II, we will give a brief overview of the setup that we plan to consider. In section III, we will analyze the linear stability of the solitary waves, utilizing different (finite difference, and Fourier, as well as Chebyshev spectral collocation) methods both for the cubic case, but also for the more general case of arbitrary exponents. We conclude that the waves should be stable for the one-dimensional cubic case, for arbitrary frequency Λ, while instabilities may *only* arise for nonlinear exponent $k > 2$ ($k = 1$ corresponds to the cubic case) and only within a certain range of Λ's. We touch upon the nature of spurious instabilities obtained in different spectra (and their identification). Finally, in section IV, we explore the nonlinear dynamics of the system. In the cubic case, we identify the growth observed as associated with (spurious) unstable eigenmodes of the linear spectrum. In the case of "super-critical" exponents with $k > 2$, the dynamics now leads to a "true" instability, but *not* one associated with collapse. Instead an oscillation around a linearly stable solution with a different frequency is observed. In a sense, it is thus concluded that the relativistic Dirac limit within the NLDE not only reduces the parametric interval (of frequency) which is subject to the collapse instability of the NLSE, but it also mitigates the catastrophic nature of such collapse in the dynamical phenomenology. Section V summarizes our findings and presents some, among the admittedly many, open challenges for future efforts.

2. Brief Theoretical Setup

The system of choice in the present context will be the Gross-Neveu model [15] in its generalized [8] form:

$$\begin{aligned} i\frac{\partial U}{\partial t} &= \frac{\partial V}{\partial x} - g(|U|^2 - |V|^2)^k U + mU, \\ i\frac{\partial V}{\partial t} &= -\frac{\partial U}{\partial x} + g(|U|^2 - |V|^2)^k V - mV. \end{aligned} \tag{1}$$

We will restrict our considerations to the one-dimensional setting, as is evident from the above. The relevant standing wave structures will be of the form: $U(x,t) = \exp(-i\Lambda t)u(x)$, $V(x,t) = \exp(-i\Lambda t)v(x)$. Then, exact solutions are analytically available in the generalized form [8, 18]

$$\begin{aligned} u(x) &= \sqrt{\frac{(m+\Lambda)\cosh^2(k\beta x)}{m+\Lambda\cosh(2k\beta x)}}\left[\frac{(k+1)\beta^2}{m+\Lambda\cosh(2k\beta x)}\right]^{1/2k}, \\ v(x) &= \mathrm{sgn}(x)\sqrt{\frac{(m-\Lambda)\sinh^2(k\beta x)}{m+\Lambda\cosh(2k\beta x)}}\left[\frac{(k+1)\beta^2}{m+\Lambda\cosh(2k\beta x)}\right]^{1/2k}. \end{aligned} \tag{2}$$

In this expression, $\beta = \sqrt{m^2 - \Lambda^2}$. In the special case of $k = 1$ the above waveforms reduce to

$$u(x) = \frac{\sqrt{2(m-\Lambda)}}{[1-\mu\tanh^2(\beta x)]\cosh(\beta x)}, \quad v(x) = \frac{\sqrt{2\mu(m-\Lambda)}\tanh(\beta x)}{[1-\mu\tanh^2(\beta x)]\cosh(\beta x)}, \quad (3)$$

with $\mu = (m-\Lambda)/(m+\Lambda)$. As discussed in [8], the relevant profiles become double-humped for Λ smaller than a critical value for every k. In what follows we will set $m = 1$ (i.e., we will measure Λ in units of m).

To analyze the linear (spectral) stability of the relevant states, we consider infinitesimal perturbations of the form:

$$U(t) = e^{-i\Lambda t}\left[u_0 + \delta(ae^{i\omega t} + c^* e^{-i\omega^* t})\right], \quad V(t) = e^{-i\Lambda t}\left[v_0 + \delta(be^{i\omega t} + d^* e^{-i\omega^* t})\right], \quad (4)$$

where δ denotes a formal small parameter. The relevant linearization equations are derived to order $\mathrm{O}(\delta)$ [by substitution of the above ansatz into Eqs. (1)] and are subsequently solved as a matrix eigenvalue problem, through the different relevant techniques (see below).

Finally, once the exact waveforms and their linear stability are identified for each scheme, the corresponding full nonlinear dynamics of the scheme is monitored by means of the solution of Eqs. (1). In that setting, key quantities for numerical monitoring are the prototypical conservation laws of the system such as the charge (squared ℓ^2 norm):

$$Q = \int \left[|U(x,t)|^2 + |V(x,t)|^2\right] dx, \quad (5)$$

and the Hamiltonian (energy) of the system in the form:

$$H = \frac{1}{2}\int \left[\left(U^* \frac{\partial V}{\partial x} - V^* \frac{\partial U}{\partial x}\right) - \frac{g}{k+1}(|U|^2 - |V|^2)^{k+1} + m(|U|^2 - |V|^2)\right] dx. \quad (6)$$

3. Numerical Linear Stability Analysis: Comparison of Different Methods

In the work [22], a subset of the present authors used a centered difference (second order) approximation to the derivatives of Eqs. (1) (as well as of the linearization equations), as a finite difference (FDM) strategy for (potentially) approximating the full NLDE results. Here, we have complemented this strategy by using spectral collocation methods. We have utilized two case examples of such methods herein: the Fourier method (Fourier Spectral Collocation Method or FSCM hereafter), which implicitly enforces periodic boundary conditions, and the (Gauss-Lobatto-) Chebyshev collocation (Chebyshev Collocation Spectral Method or CSCM for short hereafter). The latter enforces (homogeneous) Dirichlet boundary conditions. In Appendix A, we provide the basic formulation of each of our used methods.

The advantage of the FDM from a computational perspective lies in the sparseness of the resulting matrix (and the ease of applying different types of boundary conditions). We have also checked that in this setting, the boundary conditions do not significantly affect the

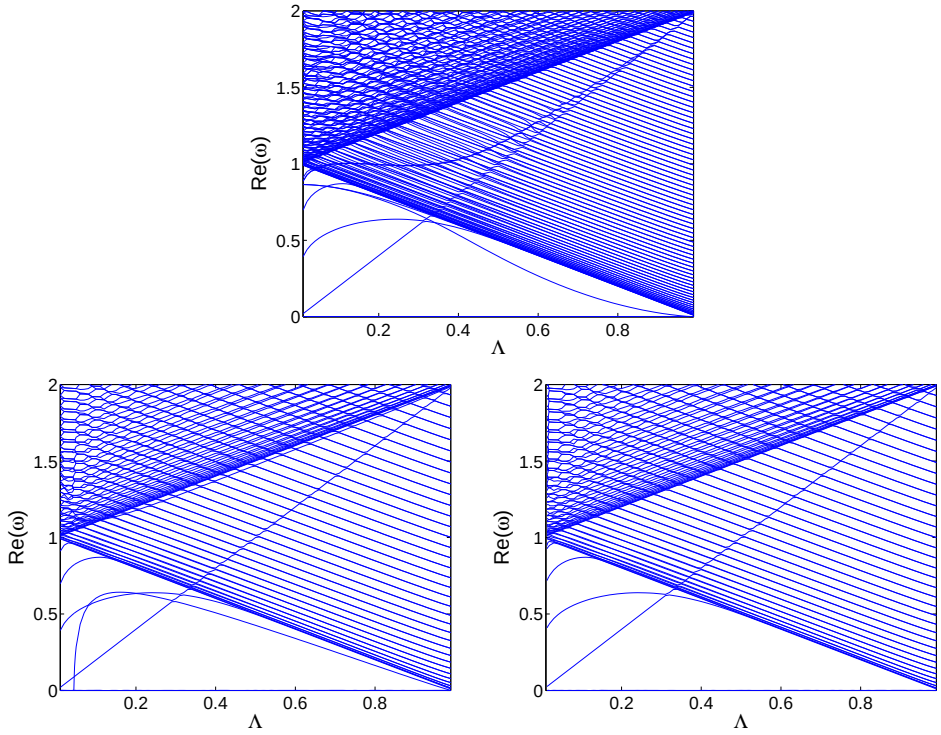

Figure 1. Real part of the eigenfrequencies for the FDM (top), FSCM (bottom left) and CSCM (bottom right). In all cases, the domain is $[-L, L]$ with $L = 40$ and the discretization parameter $h = 0.1$ (i.e. the number of grid points is $N = 800$).

results, for the domain sizes utilized. In the computations shown, we present results with $N = 800$ modes. We have checked that increasing the mode number to $N = 1200$ does not seem to qualitatively improve our findings.

In Fig. 1 we examine the dependence of the real part of the eigenfrequencies ω with respect to the frequency Λ of the solution and the three methods are compared in the cubic case of $k = 1$. As is well established (see e.g. [19]) there is an embedded mode, corresponding to $\omega = 2\Lambda$, which arises from symmetry considerations and does *not* give rise to an instability. All three methods capture this mode.

In addition to this mode, the different methods have additional modes which can be compared also e.g. with Fig. 6 of [19]. We thus find that the comparison of the FSCM with the above mentioned earlier work seems qualitatively (and even quantitatively) to yield very good agreement with the exception of a mode that seems to initially grow steeply (for small Λ) and subsequently to slowly asymptote to the band edge (as Λ increases). This mode is shown in the right panel of Fig. 2, while the left panel of the figure illustrates a prototypical example of the FSCM spectrum for $\Lambda = 0.1$. From the above panel, we can immediately infer that this mode is, in fact, spurious and an outcome of the discretization as it carries a staggered profile that cannot be supported in the continuum limit. In the left panel of Fig. 2, we can see the existence of additional spurious modes forming "bubbles" of complex eigenfrequencies. However, the fact that these bubbles are occurring at the

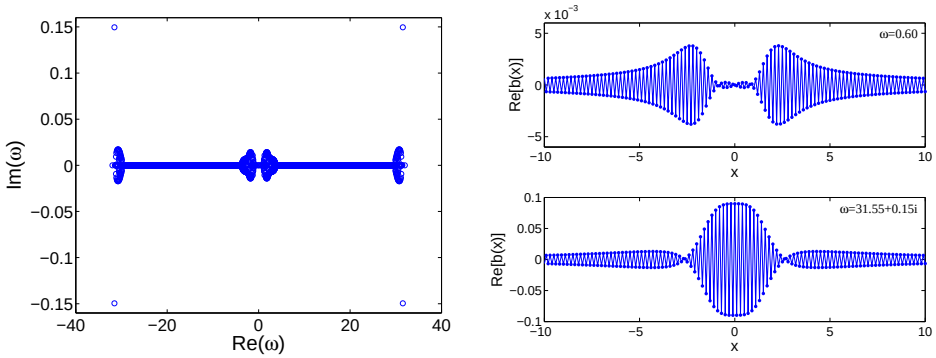

Figure 2. The left panel shows the spectral plane of a solitary wave with $\Lambda = 0.1$ with the FSCM. The typical profile of two modes corresponding to spurious eigenvalues is depicted in the right panel. In particular, we have included the mode with $\mathrm{Im}(\omega) = 0$ which does not arise in the Evans' function analysis of [19] together with the largest imaginary part eigenvalue, which is also spurious.

eigenfrequencies of the continuous spectrum assures us that these are spurious instabilities due to the finite size of the domain and ones which disappear in the $L \to \infty$, $h \to 0$ limit. This is confirmed by Fig. 3 which shows that as we decrease h (and increase the number of lattice sites, approaching the continuum limit for a given domain size) the growth rate of such spuriously unstable eigenmodes accordingly decreases.

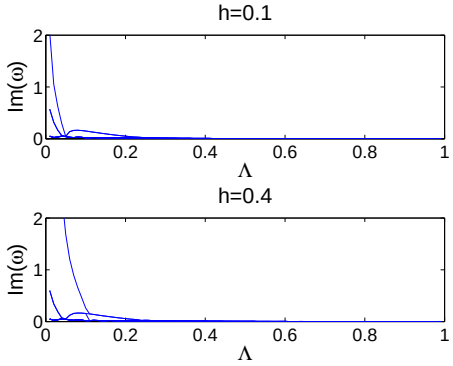

Figure 3. Imaginary part of the eigenfrequencies for the FSCM. The domain is $[-L, L]$ with $L = 40$ and the discretization parameter $h = 0.1$ or $h = 0.4$ (i.e. the number of grid points is $N = 800$ or $N = 200$).

Remarkably, the FDM spectrum of the top panel of Fig. 1 is the one that seems most "distant" from the findings of the Evans function method of [19]. While all 4 of the internal modes of the latter spectrum seem to be captured by the FDM, three additional modes create a nontrivial disparity. Two of them are in fact "benign" and maintain a frequency below the band edge of the continuous spectrum for all values of Λ. However, as explained in [22], we also observe the existence of an eigenmode embedded in the essential spectrum.

Unfortunately, this mode is accompanied by an imaginary part in the corresponding eigenfrequency and hence gives rise to a spurious, as we will indicate below, instability. While the origin of this mode starting from the so-called anti-continuum limit was thoroughly explained in [22], the persistence and especially the instability inducing nature of such a mode remains an open problem as the continuum limit is approached. Fig. 4 presents a graph analogous to Fig. 2 but for the FDM. The undesirable unstable mode, as well additional spurious modes are explicitly indicated through the eigenvector profiles of the right panel.

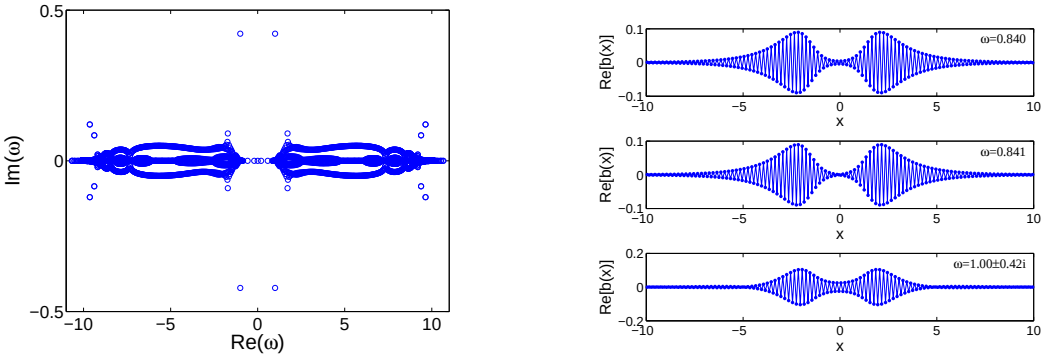

Figure 4. The left panel shows the spectral plane of a solitary wave with $\Lambda = 0.1$ with the FDM. The typical profile of three modes corresponding to spurious eigenvalues is depicted in the right panel. In particular, we have included the two modes with $\mathrm{Im}(\omega) = 0$ which do not arise in the Evans' function analysis of [19] together with the embedded spurious mode.

The scenario of the CSCM bears advantages and disadvantages in its own right. Although it gives an accurate result for the real part of the eigenfrequencies, their imaginary part grows for larger eigenfrequencies, as is also shown in Fig. 5. Additionally, as indicated in [23], approximately half of the values of the spectrum are spurious within the CSCM, so they should be excluded from consideration. Furthermore, one can observe that in this case as well, spurious instability "bubbles" arise (see the bottom panel of Fig. 5 and see also [21]), yet we have checked that these disappear in the continuum limit of $h \to 0$.

As a final aspect of the spectral considerations that we provide herein, we have examined the instability that arises e.g. from the CSCM for larger values of k. Recall that the CSCM method predicts (at least as regards the point spectrum lying below the continuous spectrum band edge of $\omega = m - \Lambda = 1 - \Lambda$ herein) that there is no instability for any Λ in the case of $k = 1$, in agreement with [19, 21]. The method identifies an instability for such point spectrum eigenvalues *only* for $k > 2$. The relevant instability predicted numerically in the $k - \Lambda$ plane is illustrated in Fig. 6. Remarkably, we note that the instability is *precisely* captured by the Vakhitov-Kolokolov criterion, i.e. it precisely corresponds to the condition [7, 14] $\frac{dQ}{d\Lambda} = 0$ for the solutions of Eq. (2). Hence, by analogy with the NLSE limit of $\Lambda \to 1$, we expect this to be an instability associated with the collapse of the latter model (however, we will observe a key dynamical difference, in comparison to the NLSE, in the next section). Nevertheless, it is relevant to point out here that the NLDE, contrary to the NLSE, does not exhibit an instability for all Λ when $k > 2$. The instability is instead

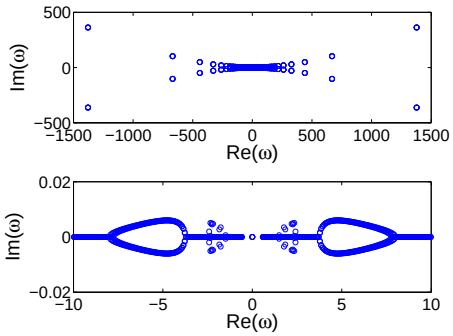

Figure 5. Spectral plane of a soliton with $\Lambda = 0.4$ with the CSCM. The bottom panel is a zoom of that on the top, illustrating the weak, spurious instabilities (which disappear as the continuum limit is approached).

limited to $\Lambda > \Lambda_c(k)$, as characterized by the curve of Fig. 6. Hence, it can be inferred that the instability is mitigated by the reletivistic limit of the NLDE.

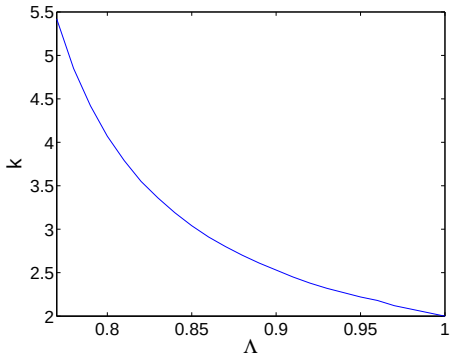

Figure 6. Exponential bifurcation loci in the k-Λ plane. Under the curve the NLDE model is linearly (spectrally) stable, while above the curve it is spectrally unstable.

4. Numerical Evolution Dynamics

We now turn our attention to the implications of the above spectral considerations to the nonlinear dynamical evolution problem. Again, we focus first on the case of $k = 1$. Given the large (yet spurious) growth rate of the CSCM modes and the spurious point spectrum instability of the FDM, for our dynamical considerations, we will restrict attention to the FSCM results. As discussed above, in that method too, there exist spurious modes which, as expected, are found to affect the corresponding dynamics. As a dynamical outcome of these modes, the solitary waves are found to be destroyed after a suitably long evolution time, although the time for this feature is controllably longer in comparison to the one

observed in [7]. This, in turn, suggests the expected stability of the solitary wave solutions, in accordance with what was proposed also in [19, 21].

As a prototypical diagnostic of the dynamical stability of the solitons, we have monitored the ℓ^2-error in a similar fashion as in [7]:

$$\mathrm{err}_2(t) = \sqrt{\int |\rho(x,t) - \rho(x,0)|^2 \, \mathrm{d}x}, \tag{7}$$

with $\rho(x,t) = |U(x,t)|^2 + |V(x,t)|^2$ being the charge density. We observe that the lifetime is longer when the frequency Λ is fixed and the domain length L is increased. This is associated with the decrease of the size of spurious instability bubbles, as we approach the infinite domain limit. Similar decrease of the growth rate is observed for a given L, when the discretization spacing h is decreased (i.e., as the continuum limit is approached), in accordance with the spectral picture of Fig. 3. In addition, if L is fixed, the lifetime is longer when Λ is increased. This is summarized in Fig. 7. This is, of course, in consonance with recent (and earlier) observations such as those of [7] (see also references therein), however, our ability to expand upon the lifetimes as the domain and discretization parameters are suitably tuned suggests that in the infinite domain, continuum limit such instabilities are absent in accordance with the spectral picture put forth by [19] (cf. also [21]). As a final comment regarding Fig. 7, we note that the growth rates observed in the figure are *consonant* with the maximal (yet spurious) instability growth identified in the corresponding spectral figures of the earlier section. This is yet another indication that this growth featured in the time dynamics is a spurious by-product of the discretization scheme, rather than a true feature of the corresponding continuum problem. Notice that decreasing the time step of the integrator Δt (we are using a Runge-Kutta with fixed step-size) also leads to a controllably smaller error as well; a demonstration of this feature is shown in Fig. 8. Let us mention in passing that while we observe this feature for large Λ, for sufficiently small Λ this trend may be reversed and higher Δt may offer more robust dynamical evolution than lower Δt. Understanding this more complex role of the time step in the evolution is worthwhile of further investigation.

In Table 1 we compare the critical time for which $\mathrm{err}_2 > 10^{-3}$ within the FSCM and the corresponding time for the algorithm used in [7] for which we have the wave frequencies $\Lambda = 0.1$ and $\Lambda = 0.5$ and different domain lengths L. As can be seen from the comparison, although in some cases (e.g. for $\Lambda = 0.5$ and $L = 50$) the observed destabilization may happen later for the scheme of [7], generally the FSCM code explored herein allows to enhance the wave lifetime, in some cases by an order of magnitude. This can be further improved by tweaking parameters such as h and the time spacing Δt, as discussed above. Hence, our conclusion is that despite the artificial instabilities existing in the spectral picture and their dynamical manifestation, it is anticipated that the continuum, real line variant of the problem is spectrally stable for all Λ in the case of $k = 1$.

Given that the solitary wave solutions of the problem with $k = 1$ (and, in fact, with any $k < 2$) are argued to be dynamically stable, we now turn our attention to the dynamics associated with the instability for $\Lambda > \Lambda_c(k)$, as per Fig. 6. Figure 9 shows the evolution of an exponentially-unstable solitary wave with $k = 3$ and $\Lambda = 0.9$. We can observe the existence of oscillations around a stable fixed point. This fixed point approximately

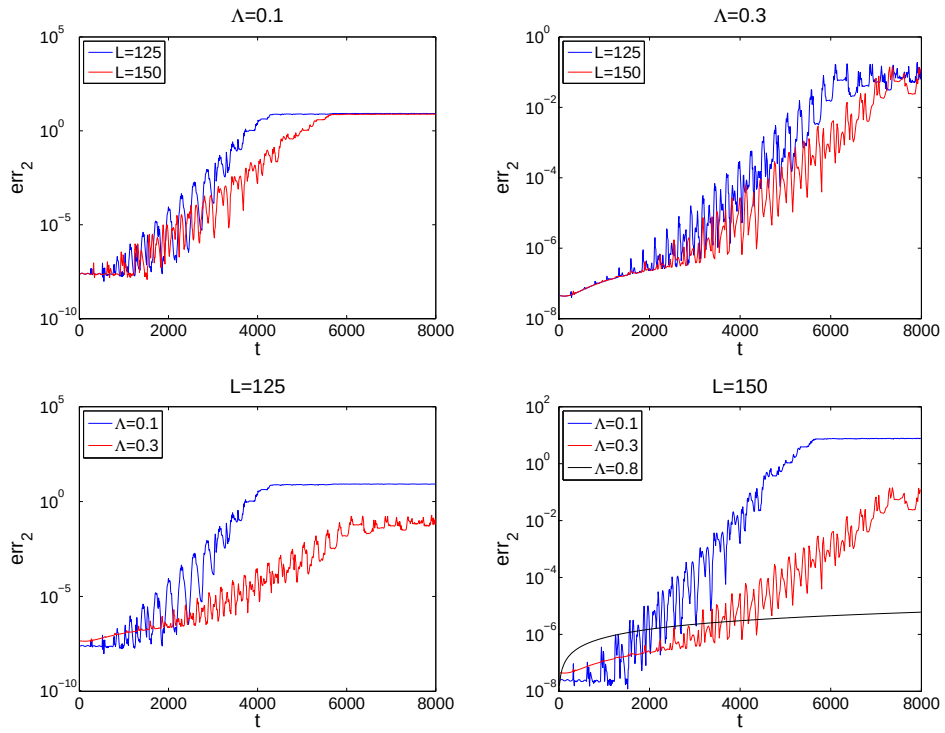

Figure 7. Norm error comparison for different domain sizes and frequencies. In every case, the time step of the integrator is $\Delta t = 0.05$.

corresponds to the soliton with frequency $\Lambda \approx 0.82$, for which the solution is spectrally stable. This is in stark contrast with the supercritical dynamics of the NLSE. There, the instability directly leads to collapse and indefinite growth of the amplitude of the solution. On the contrary, in the case of the NLDE, for any value of k for which the solution may become unstable, there exists (for the same k) an interval of spectrally stable states of the same type. Hence, the NLDE solution does not escape towards collapse but rather departs from the vicinity of the unstable fixed point solution and finds itself orbiting around a center, i.e., a stable solitary wave structure.

5. Conclusion

In the present work, we revisited the controversial issue of the spectral stability and nonlinear dynamics of stationary nonlinear wave states in the continuum nonlinear Dirac equation with arbitrary exponent k, and as a function of the standing wave frequency Λ. We offered the perspective of different spectral approaches for identifying the stability characteristics of the wave, including a finite difference method, a Fourier spectral method and a Chebyshev spectral method. We compared the findings of these different methods with earlier works (such as the Evans function based results of [19] and the Chebyshev based ones of [21]). We concluded on the basis of this comparison that the case of $k = 1$ should be spectrally stable in the infinite domain, continuum limit for this cubic case and for all settings with

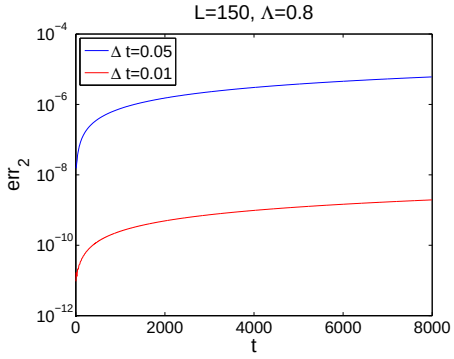

Figure 8. Norm error comparison for different time steps of the integrator, showcasing the decrease of the error as the simulation time step is decreased.

Table 1. Comparison between the critical times for which $\mathrm{err}_2 > 10^{-3}$ using the FSCM (t_2) and the SO(4) method of [7].

	$\Lambda = 0.1$		$\Lambda = 0.5$	
L	t_1	t_2	t_1	t_2
50	1220	121	5620	6614
75	1320	122	8480	8724
100	1990	122	14660	9937
125	2540	120	14660	11670
150	3120	122	14660	13560

$k < 2$, for all frequencies $\Lambda < m$ (the mass of the massive Gross-Neveu model). On the other hand, for $k > 2$, we found that an interval of instability opens, in excellent agreement with the prediction of the Vakhitov-Kolokolov criterion. However, this instability contrary to the NLSE case does not arise for all frequencies Λ, but only for an interval of $\Lambda > \Lambda_c(k)$, in accordance with the criterion. This lends support to the fact that the relativistic character of the NLDE mitigates the collapse instability of its non-relativistic NLSE analogue.

Finally, we also explored the dynamical manifestations of the instabilities. We used as our scheme of choice for exploring them the Fourier method (for reasons explained above) and found that the instabilities identified spectrally manifest themselves in the nonlinear integration dynamics of the system. However, as noted above, these instabilities could be suppressed by suitably approaching the real line, continuum limit of the problem, by suitably tuning the domain size L, the discretization spacing h and the time discretization Δt. A comparison, to that effect, with the recent results of [7] indicates that wave "destruction" times could be pushed (for similar parameter values) an order of magnitude higher attesting to the stability of the relevant coherent structures. In the case of the instability arising for

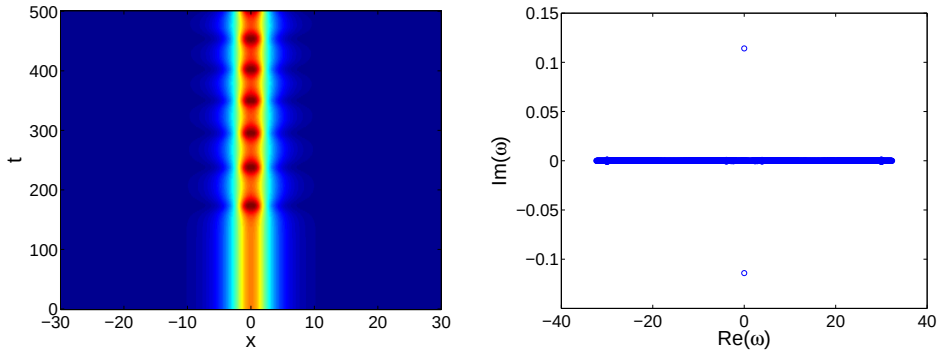

Figure 9. (Left) Time evolution of a soliton with nonlinearity exponent $k = 3$ and frequency $\Lambda = 3$. The right panel shows the spectral plane of the soliton.

$k > 2$, we observed that the dynamics of the NLDE, contrary to that of the NLSE, led to a persistent oscillation around a stable nonlinear wave (of different frequency, for the same k) rather than to collapse.

Naturally, there are still numerous intriguing open questions in this budding research theme. One important aspect to eventually understand is about the source of disparity between the different methods and why (contrary e.g. to what is known in the NLSE case) this does not go away as we approach the continuum limit in some of the relevant cases, e.g., in the finite difference method. A complementary and, arguably, more important aspect would involve seeking discretizations of the Gross-Neveu model devoid of the pathologies that we identified herein. Especially, seeking integrable-like discretizations (e.g. of the integrable massive Thirring model) that may avoid the spurious instabilities and may properly capture the continuum limit would appear an especially worthwhile cause, as it would tremendously facilitate computations and comparisons to rigorously obtained results, of which a significant and continuously growing volume of efforts is emerging. As an additional direction of interest, we note that higher-dimensional settings in the context of these models are nearly untouched from the point of view of detailed computations and comparison to theoretical predictions. Examining certain aspects even at the level of radially symmetric solutions (and general perturbations thereof) would already be a significant step in that direction. Efforts in all of these directions are presently underway and corresponding results will be reported in future publications.

Acknowledgments. P.G.K. gratefully acknowledges the support of NSF-DMS-1312856, as well as from the US-AFOSR under grant FA9550-12-1-0332, and the ERC under FP7, Marie Curie Actions, People, International Research Staff Exchange Scheme (IRSES-605096). Work at Los Alamos is supported in part by the U.S. Department of Energy. We also acknowledge Francisco R. Villatoro for his useful comments.

A Summary of Spectral Methods

We briefly discuss in this appendix the basic ingredients of the spectral methods used in the paper. For a detailed discussion on these methods, the reader is directed to [23] and

references therein.

Spectral methods arise due to the necessity of calculating spatial derivatives with higher accuracy than that given by finite difference methods. To this aim, a differentiation matrix $\mathbf{D}$ must be given together with collocation (i.e. grid) points x_i, which are not necessarily equi-spaced. Thus, if the *spectral* derivative of a function $u(x)$ needs to be calculated, it can be cast as:

$$u'(x) = \partial_x u(x) \leftrightarrow \tilde{u}' = \mathbf{D}\tilde{u}, \tag{8}$$

where $\tilde{u} = \{u_i\}$ and $\tilde{u}' = \{u_i'\}$, i.e., $u_i \equiv u(x_i)$ and $u_i' \equiv \partial_x u(x_i)$. If $x \in [-L, L]$ and the boundary conditions are periodic, the Fourier collocation can be used. In this case,

$$x_i = \frac{2L}{N}\left(i - \frac{N}{2}\right), \quad i = 1, 2, \ldots N \tag{9}$$

with N even. The differentiation matrix is

$$\mathbf{D}_{ij} = \begin{cases} 0 & \text{if } i = j, \\ \\ \frac{\pi}{2L}(-1)^{i+j} \cot \frac{x_i - x_j}{2} & \text{if } i \neq j. \end{cases} \tag{10}$$

Notice that doing the multiplication $\mathbf{D}u$ is equivalent to performing the following pair of Discrete Fourier Transform applications:

$$\mathbf{D}\tilde{u} = \mathcal{F}^{-1}\left(i\tilde{k}\mathcal{F}(\tilde{u})\right), \tag{11}$$

with $\mathcal{F}$ and $\mathcal{F}^{-1}$ denoting, respectively, the direct and inverse discrete Fourier transform [24]. The vector wavenumber $\tilde{k} = \{k_i\}$ is defined as:

$$k_i = \begin{cases} \frac{i\pi}{L} & \text{if } i < N/2, \\ \\ 0 & \text{if } i = N/2. \end{cases} \tag{12}$$

The computation of the direct and inverse discrete Fourier transforms, which is useful in simulations, can be accomplished by the Fast Fourier Transform. However, the differentiation matrix must be used for finding the stability matrix. Fourier spectral collocation can also be valid for N odd. For a detailed explanation, the reader is referred to [25].

Notice that the grid for finite differences discretization is the same as in the Fourier collocation; and, in addition, there is a differentiation matrix for the finite differences method, i.e.

$$\mathbf{D}_{ij} = \frac{N}{4L}\left(\delta_{j,i+1} - \delta_{j,i-1} + \delta_{i,1}\delta_{j,N} - \delta_{i,N}\delta_{j,1}\right), \tag{13}$$

with δ being Kronecker's delta. It is easy to observe that the Fourier spectral method basically consists of transforming the banded differentiation matrix of the finite differences method into a dense matrix, or, in other words, turning a nearest-neighbor interaction into a long-range one. The lack of sparsity of differentiation matrices is one of the drawbacks of spectral methods, especially when having to diagonalize large systems. However, they have the advantage of needing (a considerably) smaller number of grid points N for getting the same accuracy as with finite difference methods.

For fixed boundary conditions, the Chebyshev spectral methods are the most suitable ones. There are several collocation schemes, the Gauss-Lobatto being the most extensively used:

$$x_i = L\cos\left(\frac{i\pi}{N}\right), \quad i = 1, 2, \dots N, \tag{14}$$

with N being even or odd. The differentiation matrix is

$$\mathbf{D}_{ij} = \begin{cases} \dfrac{x_i}{2L(1-x_i^2)} & \text{if } i = j, \\ \dfrac{(-1)^{i+j}}{L\cos(x_i - x_j)} & \text{if } i \neq j. \end{cases} \tag{15}$$

In this case, Fourier transforms can also be used for calculating the spectral derivative, although it is more efficient to use the cosine transform as long as the function $u(x)$ is real.

The significant drawback of Chebyshev collocation is that the discretization matrix possesses a great number of spurious eigenvalues or *outliers*. They are approximately equal to $N/2$. These outliers also have a significant non-zero real part, which increases when N grows. This fact makes this method quite inefficient when performing numerical time-integration. However, it presents a higher spectral accuracy than the Fourier collocation method. Unfortunately the latter is not exempt from the existence of outliers, as shown in the text of the present paper.

References

[1] W. Thirring, Annals Phys. **3**, 91 (1958).

[2] S.Y. Lee, T. K. Kuo, and A Gavrielides, Phys. Rev. D **12**, 2249 (1975).

[3] F.M. Toyama, Y. Hosono, B. Ilyas, and Y. Nogami, J. Phys. A **27**, 3139 (1994).

[4] C. Sulem and P.L. Sulem, *The Nonlinear Schrödinger Equation*, Springer-Verlag (New York, 1999).

[5] M.J. Ablowitz, B. Prinari, and A.D. Trubatch, *Discrete and Continuous Nonlinear Schrödinger Systems*, Cambridge University Press (Cambridge, 2004).

[6] J. Xu, S. Shao and H. Tang, J. Comp. Phys **245**, 131 (2013).

[7] S. Shao, N.R. Quintero, F.G. Mertens, F. Cooper, A. Khare, and A. Saxena, Phys. Rev. E **90**, 032915 (2014).

[8] F. Cooper, A. Khare, B. Mihaila, and A. Saxena. Phys. Rev. E **82**, 036604 (2010).

[9] N. Boussaïd and S. Cuccagna, Comm. PDE **37**, 1001 (2012).

[10] D.E. Pelinovsky and Y. Shimabukuro, Lett. Math. Phys. **104**, 21 (2014).

[11] A. Contreras, D.E. Pelinovsky, and Y. Shimabukuro. ArXiv:1312.1019.

[12] D.E. Pelinovsky and A. Stefanov, J. Math. Phys. **53**, 073705 (2012).

[13] A. Comech, M. Guan, and S. Gustafson, Annal. Inst. Henri Poincaré (C) **31**, 639 (2014).

[14] A. Comech, G. Berkolaiko, and A. Sukhtayev, arXiv:1306.5150.

[15] D.J. Gross and A. Neveu, Phys. Rev. D **10**, 3235 (1974).

[16] I.L. Bogolubsky, Phys. Lett. A **73**, 87 (1979).

[17] A. Alvarez and M. Soler, Phys. Rev. Lett. **50**, 1230 (1983).

[18] F.G. Mertens, N.R. Quintero, F. Cooper, A. Khare, and A. Saxena. Phys. Rev. E **86**, 046602 (2012).

[19] G. Berkolaiko and A. Comech. Math. Model Nat. Phenom. **7**, 13 (2012).

[20] T. Kapitula and K. Promislow, *Spectral and dynamical stability of nonlinear waves*, Springer-Verlag (New York, 2013).

[21] D.E. Pelinovsky and Y. Shimabukuro, arXiv:1411.2130.

[22] J. Cuevas-Maraver, P.G. Kevrekidis, and A. Saxena, J. Phys. A **48**, 055204 (2015).

[23] J.P. Boyd, *Chebyshev and Fourier spectral methods*, 2nd. Edition. Dover (2001).

[24] L.N. Trefethen, *Spectral methods in MATLAB*. SIAM, Philadelphia (2000).

[25] R. Peyret, *Spectral methods for incompressible flow*. Springer (New York, 2002).